Jurnal Fisika Unand (JFU)
Vol. 12, No. 4, Oktober 2023, hal.628 – 638
ISSN: 2302-8491 (Print); 2686-2433 (Online)
https://doi.org/10.25077/jfu.12.4.628-638.2023

Open Access

Numerical Simulation of Bird Strike with Varied L/D Ratio in Hemispherical-ended Cylinder Bird Model Using Coupled Eulerian-Lagrangian Method

E Yuniarti[1,*], S Afandi Sitompul[1], B Aji Warsiyanto[1]
[1]Department of Aeronautical Engineering, University Aerospace Marshal Suryadarma, Jalan Protokol Halim Perdana Kusuma Komplek Bandara Halim Perdana Kusuma, Jakarta 13610, Indonesia

Info Artikel

Histori Artikel:
Diajukan: 6 June 2023
Direvisi: 11 July 2023
Diterima: 18 August 2023

Keywords:
Bird strike
Hemispherical-ended cylinder
Coupled Eulerian-Lagrangian method
Length-to-diameter ratio

Penulis Korespondensi:
Endah Yuniarti
Email: eyuniarti@unsurya.ac.id

ABSTRAK

This research studies the numerical simulation of the finite element method for bird strike using a hemispherical-ended cylinder bird model with varying length-to-diameter (L/D) ratio, namely 1.4; 1.5; 1.6; 1.7; 1.8; 1.9; and 2.0. Birds are modelled with elastic, plastic, and hydrodynamic behaviour. The bird model uses the Coupled Eulerian-Lagrangian (CEL) method with impact speeds of 100 ms^{-1}, 200 ms^{-1}, and 300 ms^{-1}. The CEL method avoids the disadvantages of the Lagrangian method in modeling soft body objects due to mesh distortions caused by high-speed impacts, which can lead to computational difficulties and negative volume. The simulation results show that the Hugoniot pressure value is around 15-36 times higher than stagnation pressure in L/D 1.4; 14-36 times in L/D 1.5; 13-30 times in L/D 1.6; 12-32 times in L/D 1.7; 12-26 times in L/D 1.8; 13-30 times in L/D 1.9; and 13-29 times in L/D 2.0. It was found that the highest Hugoniot and stagnation pressure is in L/D 1.5 and 1.8, while the lowest Hugoniot and stagnation pressure is in L/D 2.0 and 1.5, respectively. In addition, the error of the numerical results of the average Hugoniot and stagnation pressure value compared to the analytic was 2.9% and 7%, respectively.

I. INTRODUCTION

Birds often collide with aircraft when operating close to airports, especially during take-off and landing. In general, all components of the aircraft that are in direct contact with birds have the potential to experience a collision, for example the leading edges of the wings and tail (empennage), windshield in the cockpit, radome, landing gears, engines, and rotors. According to an FAA report (Dolbeer *et al.*, 2019) between 1990 and 2018, there were 214,048 bird strikes in the United States and aircraft registered in the United States abroad. Therefore, bird strikes are one of the biggest threats to aviation safety, both for fixed-wing and propeller aircraft.

With the aim of developing surrogate bird models for use in bird-stricken experiments, the physical behavior of birds in the bird-slash phenomenon has been investigated since the 1960s (McNaughtan, 1964) (Alcock and Collin, 1969) (Peterson and Barber, 1976) (Wilbeck, 1978)(Wilbeck and Rand, 1981) (Barber *et al.*, 1978). The investigation showed a pressure response consisting of (a) a sharp rise to peak (Hugoniot pressure), (b) pressure decay, and (c) a steady pressure or stagnation pressure (Wilbeck, 1978). It was found that birds behave essentially like liquids during the bird strike phenomenon. Thus, surrogate birds are usually modeled using gelatin which is able to provide near-bird behavior and fluid-like behavior can be simulated by hydrodynamic models (Peterson and Barber, 1976) (Wilbeck, 1978). In general, surrogate birds allow for increased productivity in hit-bird experiments compared to real birds because of the lack of dependence on individual species, mass, and shape-specific (e.g. age and sex), heterogeneous material properties, difficulty in positioning against targets, and controllability attitude of birds during collision (Nizampatnam, 2007) (Vignjevic *et al.*, 2013).

Currently, analysis by experimental and numerical methods is used to investigate the resistance of aircraft structures when receiving impact loads from the bird crash phenomenon. The high cost of conducting experimental testing has given great interest to numerical method analysis. According to Civil Aviation Safety Regulation (CASR) 25,631 (Republic Indonesia Ministry of Transportation, 2014) the bird strike test can be replaced with a precise numerical analysis as long as the results have been validated against the aircraft structure.

The Lagrangian, Coupled Eulerian-Lagrangian (CEL), and Smooth Particle Hydrodynamic (SPH) methods are used in bird impact simulations to model bird. Numerous studies indicated the advantages of using the CEL method for modeling bird. The Coupled Eulerian-Lagrangian (CEL) method can illustrate the physical behavior of birds in the phenomenon of bird strikes (Heimbs, 2011). CEL is a numerical method involving space (volume) as the deformation area of a material. Figure 1 shows an example of a bird strike simulation on a rigid plate with the CEL bird model (Heimbs, 2011). In this space, meshing and material properties of fluids (fluids) are applied. The CEL method avoids the disadvantages of the Lagrangian method in modeling soft body objects due to mesh distortions caused by high-speed impacts, which can lead to computational difficulties and negative volume. Compared to the SPH method, the modeling of the CEL method appears more realistic for modeling the deformation behavior of birds.

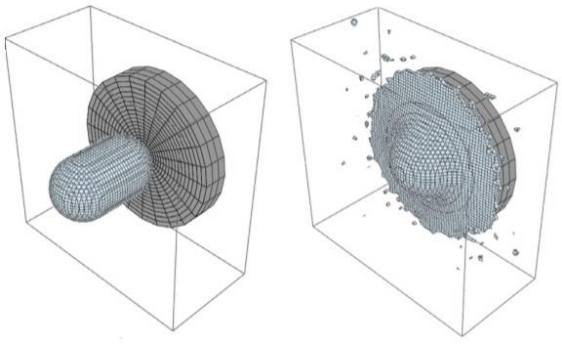

Figure 1 Bird hit simulation on rigid plate with CEL bird model

II. METHOD

Lavoie et al. (2009) stated that the Lagrangian method is inappropriate for bird-strike modeling due to pressure loss, mass loss, and inaccurate radial pressure distribution. The above-mentioned problems were resolved by using refined mesh (however increased solution time). Since at high pressures, the bird body behaves like a fluid, the Eulerian approach which is prevalent in modeling fluid dynamic problems would be helpful. In this method, a fixed void mesh is created in the space, and some of the cells are filled by bird material at the points where the bird must be present. As the bird material travels into the space, some cells become hollow and some others become filled with the bird material.

Previously, it was investigated in (Yuniarti & Sitompul, 2019) that the effect of hemispherical-ended cylinder geometry with a difference in L/D ratio of 1.4; 1.6; 1.8; and 2.0 using the Lagrangian method. It was found that the peak pressure value was about 10-19 times higher than the stagnation pressure at an L/D ratio of 1.4; 8-18 times at L/D 1.6; 9-17 times at L/D 1.8; and 4-16 times at L/D 2.0. Yuniarti et al (2020) also conducted research on the effect of hemispherical-ended cylinder geometry with a difference in L/D ratio of 1.5; 1.7; and 1.9 using the Smoothed Particle Hydrodynamics (SPH) method. It was found that the peak pressure value was about 14-25 times higher than the stagnation pressure at an L/D ratio of 1.5; 12-25 times at L/D 1.7; and 11-34 times at L/D 1.9.

It is necessary to compare the results using other methods in order to obtain a method that has advantages in terms of impact pressure values, both peak pressure or Hugoniot (P_H) and stagnation (P_s). Therefore, this study aims to obtain impact stresses based on differences in bird geometry. Mathematically, the Hugoniot pressure and stagnation equations are written as follows:

$$P_H = \rho_0 u_0 u_s \tag{1}$$

$$P_S = \frac{1}{2}\rho_0 u_0^2 \tag{2}$$

where ρ_0 is the initial density of the bird, u_0 and u_s are the impact velocity and shock wave respectively, In the form of a curve, the pressure profile when a bird strike occurs can be seen in Figure 2. The total collision duration can be determined using the following equation:

$$t_d = \frac{L}{u_0} \tag{3}$$

where L is bird length.

The first, and yet the most common, approach to model the bird is the Lagrangian method. The Lagrangian method is the default approach for discretizing solid parts in FE packages. This method uses the material coordinates as the reference, i.e. the nodes of the mesh are attached to the particles of the material. This model is able to follow the distortions of the bird material, and to some extent, the break-up of bird material into debris (Stoll & Brockman, 1997). However, there are several drawbacks in Lagrangian bird modeling. Since the nodes of the FE model are attached to the material, if the material is deformed greatly, some of the elements become highly distorted. As a result, the smallest dimension of the elements becomes very small, which in turn decreases the solution time step as well. The huge drop in the time step duration significantly increases the number of required time steps, and as a result the solution time increases (Hedayati & Ziaei-Rad, 2013b).

In the CEL method, the mesh remains in space and the material flows through the mesh as shown in Figure 3, so that stability problems due to element distortion do not occur. This method is especially used for fluid materials. The drawback of this method is that the deformation of the material is limited by space and the results depend on the size of the elements, so it is necessary to use a relatively large domain size and a fine mesh to obtain accurate results (Heimbs, 2011). However, these limitations are tolerated by the accuracy and deformation behavior of bird materials which are more realistic than the Lagrangian and SPH methods.

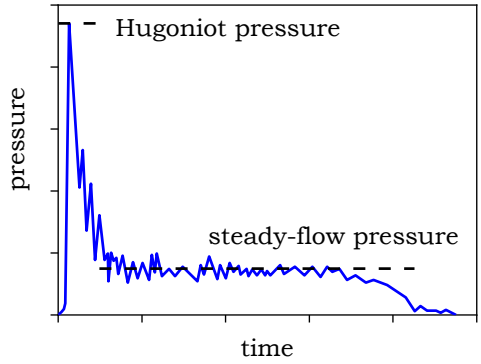

Figure 2 Impact stress profile on bird strike phenomenon

Simulations were carried out using the Abaqus/CAE finite element application to determine the effect of differences in the geometry of the bird model in the form of a hemispherical-ended cylinder (a cylinder with both ends of a hemispherical) on the impact pressure distribution. The hemispherical-ended cylinder shape was chosen because (Hedayati and Sadighi, 2015) had performed a simulation to compare the pressure values between bird shapes (straight-ended cylinder, hemispherical-ended cylinder, ellipse, and sphere) and experiments conducted by (Wilbeck, 1978). The result is that the hemispherical-ended cylinder shape is closest to the experimental pressure value (Wilbeck, 1978). For modelling using the CEL method, three parts are needed consisting of birds, plates, and domains (space) as shown in Figures 4 and 5. Domain is the space where material flows when it undergoes movement and deformation.

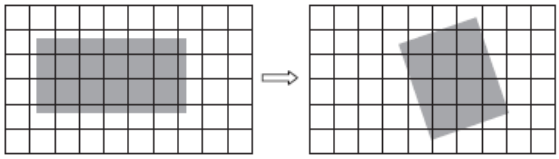

Figure 3 Material flow through the mesh in the Eulerian method

Table 1 Bird Dimension and Eulerian Domain for varied L/D ratio

Ratio (L/D)	Bird		Domain		
	Length, L (mm)	Diameter, D (mm)	Length, P (mm)	Width, W (mm)	Height, H (mm)
1,4	185	132	139	69,5	69,5
1,5	193	128	135	67,5	67,5
1,6	200	125	132	66,0	66,0
1,7	207	122	129	64,5	64,5
1,8	214	119	126	63,0	63,0
1,9	221	116	123	61,5	61,5
2,0	228	114	121	60,5	60,5

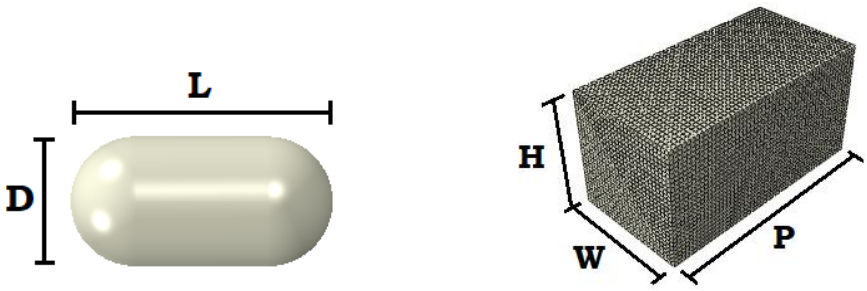

(a) (b)

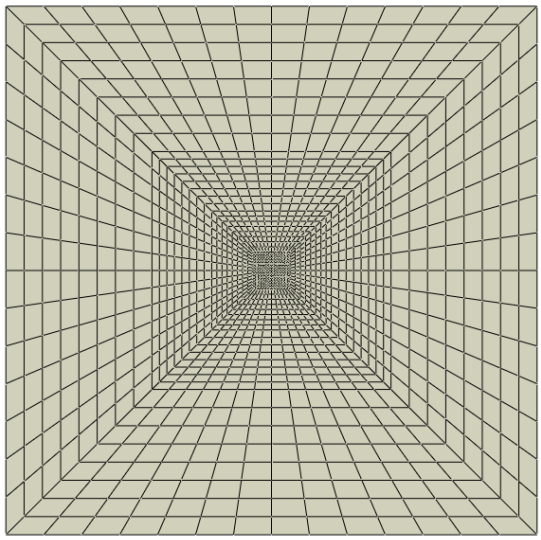

(c)

Figure 4 Part Models: (a) Bird, (b) Eulerian Domain, and (c) Plate

The difference in bird geometry is based on the ratio of length to diameter (L/D) as shown in Figure 4(a), which is 1.4; 1.5; 1.6; 1.7; 1.8; 1.9; and 2.0. Details of the dimensions of the bird model for L/D and domain differences are shown in Table 1. The mass of the bird was determined at 1.82 kg based on a CASR of 25,571. This study aims to determine the value of Hugoniot pressure and stagnation for each bird geometry which is then averaged and compared with analytical pressure. When a bird strike occurs at high speed, the bird material has a fluid-like behavior. To model the hydrodynamic response accurately, the hydrodynamic fluid material defined by the Equation of State (EOS) Tabular was used in this study. EOS Tabular defines the relationship between pressure and density ratio (before and after collision) (SIMULIA, 2011). Mathematically, the EOS Tabular is written as follows:

$$p = f_1(\varepsilon_V) + \rho_0 f_2(\varepsilon_V) E_m \tag{4}$$

where $f_1(\varepsilon_V)$ and $f_2(\varepsilon_V)$ are logarithmic functions of the volume strain ($\varepsilon_V = \ln(\rho_0/\rho)$) and E_m is the internal energy per unit mass. However, the effect of internal energy on pressure is negligible when dealing with hydrodynamic collisions. Therefore, $f_2(\varepsilon_V) = 0$ so that $p = f_1(\varepsilon_V)$. The EOS Tabular defines the curve in Figure 6 that requires only the natural logarithm of the density ratio (ρ_0/ρ).

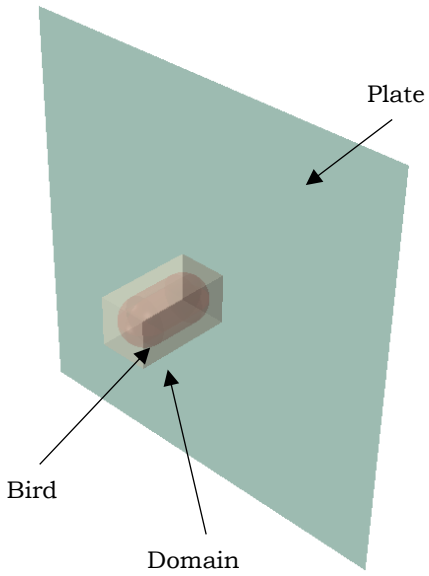

Figure 5 Bird Strike Modeling Assembly

Native birds have porosity or internal cavities between body organs, thereby reducing the density value. The effect of the porosity is represented by an average density in the range of 900-950 kg/m^3. Porosity has a significant influence on the resulting peak pressure. For example, a porosity of 0.1 can reduce peak stresses by up to 50% compared to a porosity of 0%. In this study, bird material with 0% porosity was used to obtain conservative results. In the case of 0% porosity, the value of u_s can be calculated by the linear Hugoniot equation for water (Wilbeck, 1978), namely:

$$u_s = c_0 + 2u_0 \tag{5}$$

with c_0 = 1482.9 ms^{-1} which defines the speed of sound in birds at the start of impact. The mechanical properties and tabular EOS for bird materials are shown in Tables 2 and 3, respectively.

Meshing is significantly simplified for the approach using the CEL method because the bird part does not require a mesh. A uniform mesh (same size) is applied to the Eulerian domain with element type EC3D8R so that the bird geometry is completely filled with the mesh and material constraints of the Eulerian domain. This can be achieved by making the Eulerian mesh immobile and its dimensions capable of covering the entire bird movement path from start to finish of the simulation. Material in the Eulerian domain will be filled into the bird part by a technique based on the volume fraction of the bird material in each Eulerian element. The mesh for the Eulerian domain part is made with different sizes depending on the L/D ratio, which is 2.5 – 5 mm, resulting in 28,392 – 233,280 elements. No constraints are used on the movement of the Eulerian mesh. The Volume Fraction Tool is used to create a discrete field that defines the bird's initial location. High accuracy should be used for field creation. This arrangement provides a good balance between analytical accuracy and computational efficiency.

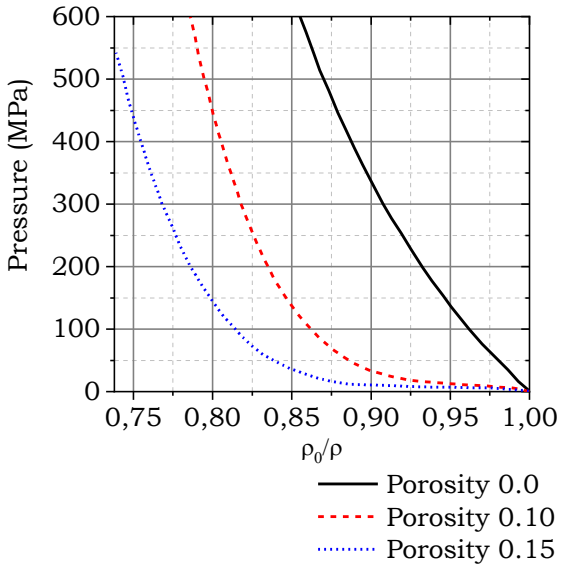

Figure 6 Hugoniot pressure relationship with density ratio in homogeneous bird material.

Table 2 Bird material mechanical property

Parameters	Value
Density	938 kg.m^{-3}
Shear Modulus	10 MPa
Yield Strength	0,1 MPa
Hydrostatic Strength	2,75 MPa

Table 3 EOS Tabular Parameters

No	f_1 (MPa)	ε_V	No	f_1 (MPa)	ε_V
1	0	0	14	263,29	-0,088
2	15,82	-0,007	15	289,34	-0,095
3	32,56	-0,014	16	315,39	-0,100
4	51,17	-0,021	17	342,37	-0,107
5	68,85	-0,028	18	370,29	-0,113
6	87,45	-0,035	19	399,13	-0,119
7	106,06	-0,042	20	429,83	-0,126
8	127,46	-0,049	21	460,53	-0,132
9	147,93	-0,055	22	493,09	-0,138
10	168,40	-0,062	23	526,59	-0,144
11	191,66	-0,068	24	561,01	-0,150
12	213,98	-0,075	25	595,43	-0,156
13	238,17	-0,081			

A square steel plate is modelled as a target by the Lagrangian method. The plate has dimensions of 1000x1000 mm and a thickness of 50.8 mm [5] which is fixed at the edges. The mechanical properties of the steel material consist of a density of 7,800 kg.m^{-3}, a modulus of elasticity of 207 GPa, and a Poisson's ratio of 0.3. The slab meshing produces 1,540 elements. The mesh size is made tighter (smaller) in the collision centre area to maintain accuracy of results and reduce computation time. The element type is modelled as a 4-node shell continuum (S4R) element with 5 integration points along the thickness direction. The simulation time used varies depending on the length and speed calculated using Equation 4. The contact algorithm used is general contact to define all contacts between parts.

III. RESULTS AND DISCUSSION

The simulation of bird strike using CEL modelling has been successfully carried out. The stages of bird deformation based on time intervals are shown in Figure 7. The figure shows the deformation process using the largest domain size from the size shown in Table 1. It is intended to provide an easier visualization understanding of the deformation for the CEL method approach. Hugoniot pressure and stagnation are used as analytical parameters which are obtained by dividing the total contact force (via the output parameter, CFNM) by the contact area (via the output parameter, CAREA) each time (time step). This value is obtained from the location around the centre of impact by making a reference set of four elements measuring 5x5 mm for each element. For the Hugoniot pressure, the peak value is determined, while the stagnation pressure is obtained by averaging the pressure in the time interval of $1/3\ t_d$ until $2/3\ t_d$, which had been suggested as representative of the steady flow phase (Airoldi and Cacchione, 2006). More specifically, this is accomplished by first numerically integrating the pressure-time history between the time instances $1/3\ t_d$ and $2/3\ t_d$ and then dividing the result by $1/3\ t_d$.

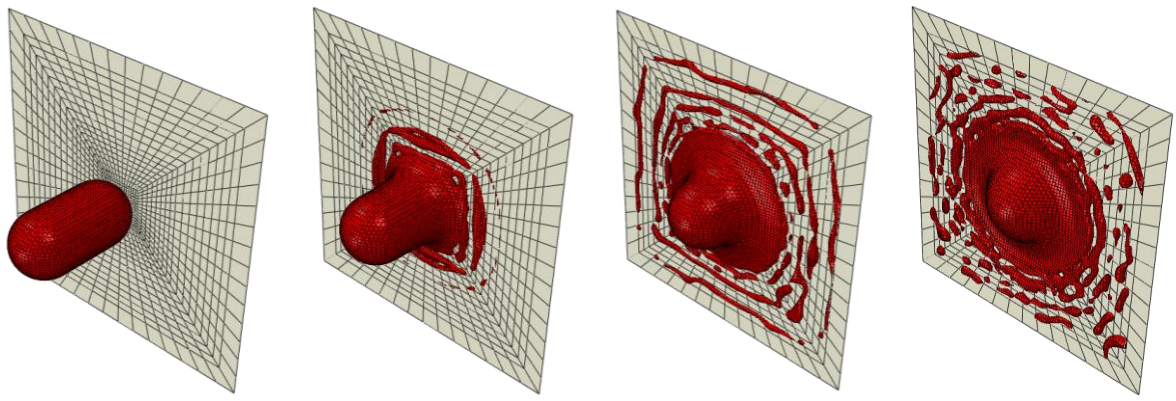

(a) (b) (c) (d)

Figure 7 Deformation of birds at 2.0 L/D ratio at 300 ms^{-1} based on time interval: (a) 0 ms, (b) 0.19 ms, (c) 0.38 ms, (d) 0.57 ms

The output results are shown in the form of the pressure versus time curve shown in Figures 8-14 for the different L/D ratios. Overall, the pattern or trend of the curve is almost the same, namely it increases in height at the beginning of the impact (Hugoniot pressure) and tends to be constant over time after (stagnation pressure). In one figure there are three curves for different speeds at the same L/D ratio. It can be seen that the curve pattern for the speed of 100 ms^{-1} is longer than the speed above it (200 and 300 ms^{-1}) because the higher the impact velocity, the lower the collision duration. In addition to the pressure results shown in the form of a curve, the pressure values are summarized in tables for the respective Hugoniot and stagnation pressures as shown in Table 4.

It can be seen that the average values of Hugoniot pressure and stagnation for the overall L/D ratio of the bird model are 165,697 and 5,309 MPa at speeds of 100 ms^{-1}, 359.513 and 19.131 MPa at 200 ms^{-1}, and 575.176 and 44.711 MPa at speeds of 300 ms^{-1}, respectively. The results of the average value of the pressure, both Hugoniot and stagnation will then be calculated the value of the percentage error based on the analytical value. To determine the value of Hugoniot pressure and analytical stagnation, Equations 1 and 2 are used. Comparison of error values between numerical and analytical pressures is shown in Table 5.

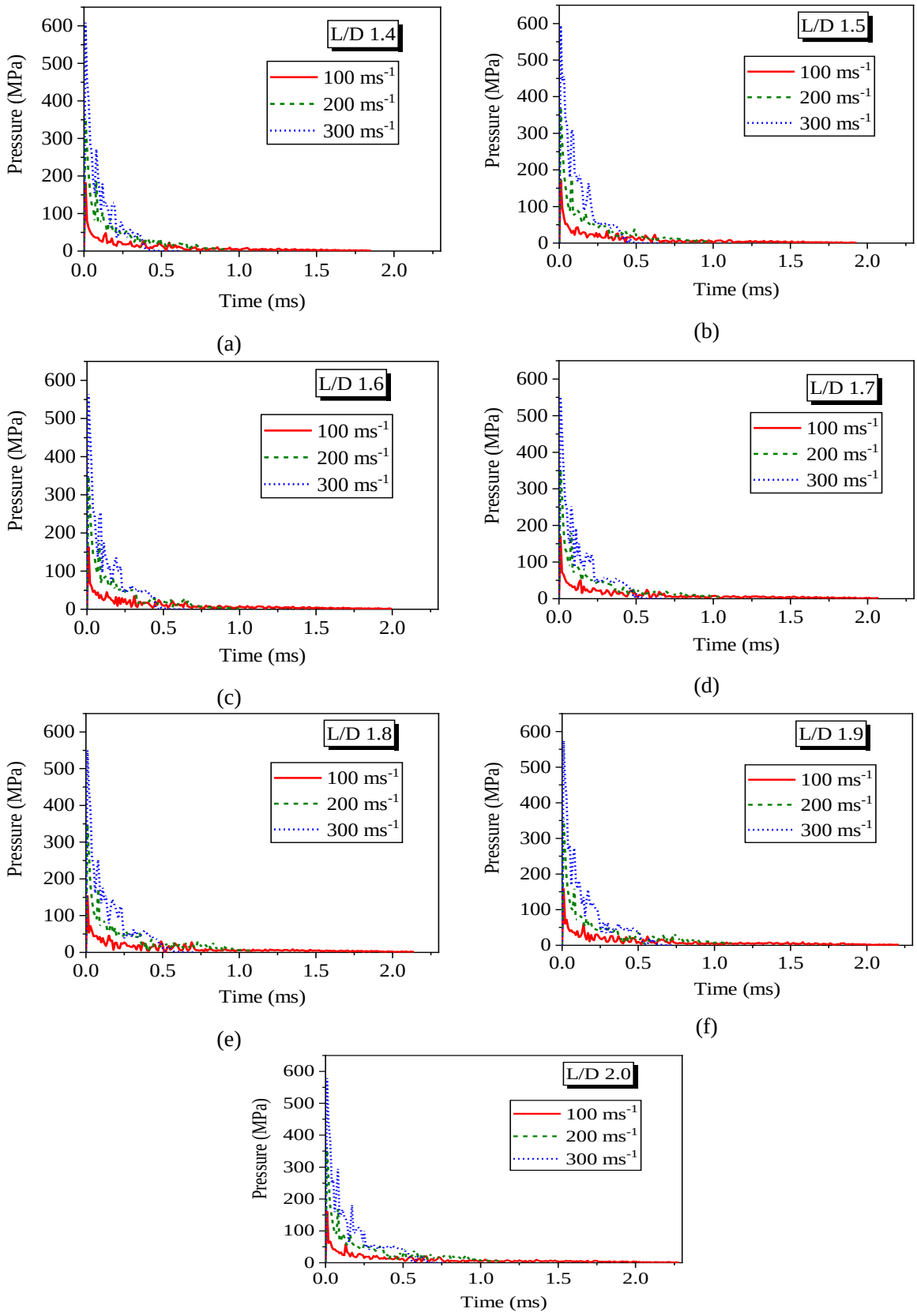

Figure 8 Impact pressure curve against impact time for L/D Ratio (a) 1.4, (b) 1.5, (c) 1.6, (d) 1.7, (e) 1.8, (f) 1.9, dan (g) 2.0

Table 4 Hugoniot Pressure Value based on varied L/D ratio and Impact Velocity

L/D	Hugoniot Pressure (MPa)			Stagnation Pressure (MPa)		
	impact velocity 100 ms^{-1}	impact velocity 200 ms^{-1}	impact velocity 300 ms^{-1}	impact velocity 100 ms^{-1}	impact velocity 200 ms^{-1}	impact velocity 300 ms^{-1}
1.4	181.375	365.336	609.466	5.099	21.760	40.621
1.5	173.155	372.722	594.695	4.847	19.480	43.462
1.6	163.378	350.152	565.741	5.401	17.841	45.027
1.7	169.748	354.254	552.524	5.285	18.731	46.810
1.8	153.630	350.149	550.505	5.843	17.390	45.851
1.9	157.938	359.892	574.094	5.195	18.093	45.274
2.0	160.658	364.084	579.209	5.495	20.623	45.934
Average	165.697	359.513	575.176	5.309	19.131	44.711

Based on the curves and pressure values in Figures 8 as well as Table 4, it can be seen that the highest Hugoniot pressure is at L/D 1.4, which is 609.466 MPa, while the lowest Hugoniot pressure is at L/D. 1.8, which is 153.630 MPa. The highest stagnation pressure is at L/D 1.7, which is 46.81 MPa, while the lowest stagnation pressure is at L/D 1.5, which is 4.847 MPa. Trend of the curve (see Figs. 8) shows that the impact pressure increases rapidly, reaches a peak at the beginning of the collision which then decreases until it tends to be constant with time. On average for each speed, the highest and lowest Hugoniot pressure for each L/D is located at L/D 1.4 and 1.8, respectively, while the highest and lowest stagnation pressure for each L/D lies at L/D 2.0 and 1.4.

Table 5 Comparison of Hugoniot Pressure and Stagnation Pressure Values between Analytical and Numerical Methods

Velocity (ms^{-1})	Hugoniot Pressure (MPa)			Stagnation Pressure (MPa)		
	Analitycal	Numerical	*Error* (%)	Analitycal	Numerical	*Error* (%)
100	157.86	165.697	5.0	4.69	5.309	13.2
200	353.23	359.513	1.8	18.76	19.131	2.0
300	586.13	575.176	-1.9	42.21	44.711	5.9
Average			2.9	Average		7.0

IV. CONCLUSION

The simulation results for hemispherical-ended cylinder-shaped bird geometry show the Hugoniot pressure value of about 15-36 times higher than the stagnation pressure at L/D 1.4; 14-36 times at L/D 1.5; 13-30 at L/D 1.6; 12-32 times at L/D 1.7; 12-26 times at L/D 1.8; 13-30 times at 1.9; and 13-29 times at L/D 2.0. The physical behaviour of the deformation or spread of bird material during a collision can be well illustrated and there are no mesh distortion problems in the bird model from the beginning to the end of the simulation. The mean error values for Hugoniot pressure and stagnation at speeds of 100 ms-1, 200 ms-1, and 300 ms-1, respectively, were 2.9% and 7.0%, respectively. Thus, the bird strike simulation approach using the CEL method can be said to be good when compared to the results of the Hugoniot pressure and stagnation values from the analytical method.

ACKNOWLEDGEMENT

The author would like to thank Lembaga Penelitian dan Pengabdian Kepada Masyarakat (LPPM) Universitas Dirgantara Marsekal Suryadarma (Unsurya).

REFERENCE

Alcock, A.W.R. and Collin, D.M. (1969), "The Development of a Dummy Bird for use in Bird Strike Research", No. Technical Report, National Gas Turbine Establishment.

Barber, J.P., Taylor, H.R. and Wilbeck, J.S. (1978), "Bird Impact Forces and Pressures on Rigid and Compliant Targets", No. Technical Report AFFDL-TR-77-60. University of Dayton Ohio Research Institute. Air Force Flight Dynamics Laboratory.

Dolbeer, R.A., Begier, M.J., Miller, P.R., Weller, J.R. and Anderson, A.L. (2019), "Wildlife Strikes to Civil Aircraft in the United States 1990-2018", *Federal Aviation Administration. National Wildlife Strike Database.*

Hedayati, R. and Sadighi, M. (2015), *Bird Strike: An Experimental, Theoretical and Numerical Investigation*, *Woodhead Publishing*, doi: 10.1016/C2014-0-02336-2.

Heimbs, S. (2011), "Computational Methods for Bird Strike Simulations: A Review", *Computers and Structures*, Elsevier Ltd, Vol. 89 No. 23–24, pp. 2093–2112, doi: 10.1016/j.compstruc.2011.08.007.

McNaughtan, I.I. (1964), "The Resistance of Transparencies to Bird Impact at High Speeds", *Aircraft Engineering and Aerospace Technology*, doi: 10.1108/eb033964.

Nizampatnam, L.S. (2007), "Models and Methods for Bird Strike Load Predictions", *Wichita State University*.

Peterson, R.L. and Barber, J.P. (1976), "Bird Impact Forces in Aircraft Windshield Design", No. Technical Report AFML-Tr-76-54, AFML, University of Dayton Research Institute, Dayton, Ohio, USA.

SIMULIA. (2011), *A Strategy for Bird Strike Simulations Using Abaqus / Explicit*.

Vignjevic, R., Orłowski, M., De Vuyst, T. and Campbell, J.C. (2013), "A Parametric Study of Bird Strike on Engine Blades", *International Journal of Impact Engineering*, Vol. 60, pp. 44–57, doi: 10.1016/j.ijimpeng.2013.04.003.

Wilbeck, J.S. (1978), "Impact Behavior of Low Strength Projectiles", No. Technical Report AFML-TR-77-134. Air Force Materials Laboratory. Wright-Patterson Air Force Base, Ohio, 45433, USA.

Wilbeck, J.S. and Rand, J.L. (1981), "The Development of a Substitute Bird Model", *Journal of Engineering for Gas Turbines and Power*, Vol. 103 No. 4, pp. 725–730, doi: 10.1115/1.3230795.